Langmuir
Article
pubs.acs.org/Langmuir

Dynamic Mobility of Rodlike Goethite Particles

R. A. Rica, M. L. Jiménez, and A. V. Delgado*

Department of Applied Physics, School of Sciences, Campus Fuentenueva University of Granada, 18071 Granada, Spain

Received April 20, 2009. Revised Manuscript Received June 8, 2009

In this work we consider how the spheroidal shape of colloidal particles and their concentration in suspension influence their electrokinetic properties in alternating (ac) electric fields, in particular, their electrophoretic mobility, traditionally known as dynamic mobility in the case of ac fields. Elaboration of a formula for the mobility is based on two previous models related to the electrokinetic response of spheroids in dilute suspensions, completed by means of an approximate formula to account for the finite concentration of particles. At the end, semianalytical formulas have been obtained in the form of the classical Helmholtz−Smoluchowski equation for the mobility with three frequency-dependent factors, each dealing with inertia relaxation, electric double layer polarization and volume fraction effects. The two resulting expressions differ basically in their consideration of double layer polarization processes, as one considers only Maxwell−Wagner−O'Konski polarization (related to the mismatch between the conductivities of the particles plus their double layers and the liquid medium), and the other also includes the concentration polarization effect. Since in the frequency range typically used in dynamic mobility measurements the latter polarization has already relaxed, both models are capable of accounting for the dynamic mobility data experimentally obtained on elongated goethite particles in the 1−18 MHz frequency range. Results are presented concerning the effects of volume fraction, ionic strength, and pH, and they indicate that the models are good descriptions of the electrokinetics of these systems, and that dynamic mobility is very sensitive not only to the zeta potential of the particles, but also to their concentration, shape, and average size, and to the stability of the suspensions. The effects of ionic strength and pH on the dynamic mobility are very well captured by both models, and a consistent description of the dimensions and zeta potentials of the particles is reached. Increasing the volume fraction of the suspensions produces mobility variations that are only partially described by the theoretical calculations due to the likely flocculation of the particles, mainly associated with the fact that goethite particles are not homogeneously charged, with attraction between positive and negative patches being possible.

Introduction

Concentrated suspensions of colloidal particles find applications in a wide variety of fields, including paints, ceramics, drug dispersions, soils, or food processing, to mention a few.[1] Very often, such applications need procedures (either online or in the quality control laboratories) for testing the physical state of the suspension, particularly concerning its stability, particle size, particle charge, and so forth. Light scattering techniques are very suited to be used in online determinations, but they are applicable to dilute or slightly concentrated systems, in spite of significant improvements recently described.[2]

Methods based on the determination of some electrokinetic properties of the dispersed particles are classical tools that are gaining acceptance and applicability, especially since the introduction of electroacoustic techniques.[3] These permit the evaluation of the frequency spectrum of the so-called dynamic electrophoretic mobility, u_e, a complex quantity that can be considered as the alternating current (ac) counterpart of the direct current (dc) or standard electrophoretic mobility. Interestingly, the electroacoustic response is a collective one and the measurements can be carried out without the need of diluting the sample, thus altering its state.[4−7] In addition, the existing experimental techniques provide very useful information on the in situ particle size distribution, making use of the high-frequency relaxation of the mobility or the attenuation of an acoustic wave through the suspension.

The mobility spectrum is determined by the properties of the particle itself (like size, shape, chemical composition, and surface charge) and by the polarization state of the ionic atmosphere around the particle (its electrical double layer or EDL). The problem has been solved extensively for spherical particles,[5−8] but fewer works have been devoted to the evaluation of the dynamic mobility of nonspherical particles. One of the mathematical complications of the solution in the case of such geometries is the description of the polarization of the EDL of the particles in the presence of an alternating electric field. This has been solved analytically by Shilov et al.[8,9] and numerically by Fixman,[10] although, unfortunately, experimental tests of these descriptions are practically nonexistent. Furthermore, the calculation of the dynamic mobility of such particles needs the knowledge of the unsteady (oscillatory) Stokes resistance, which is not solved for

*Corresponding author. Address: Departamento de Física Aplicada, Facultad de Ciencias, Campus Fuentenueva, Universidad de Granada, 18071 Granada, Spain. Fax: +34-958 24 32 14. E-mail: adelgado@ugr.es.

(1) McKay, R. B., Ed. *Technological Applications of Dispersions*; Marcel Dekker Inc.: New York, 1994.
(2) Medebach, M.; Moitzi, C.; Freiberger, N.; Glatter, O. *J. Colloid Interface Sci.* **2007**, *305*, 88–93.
(3) Hunter, R. J. *Colloids Surf., A* **1998**, *141*, 37–65.
(4) O'Brien, R. W. *J. Fluid Mech.* **1988**, *190*, 71–86.
(5) O'Brien, R. W.; Cannon, D. W.; Rowlands, W. N. *J. Colloid Interface Sci.* **1995**, *173*, 406–418.
(6) Rider, P. F.; O'Brien, R. W. *J. Fluid Mech.* **1993**, *257*, 607–636.
(7) Ahualli, S.; Jimenez, M. L.; Delgado, A. V.; Arroyo, F. J.; Carrique, F. *IEEE Transactions on Dielectrics and Electrical Insulation* **2005**, *13*, 657–663.
(8) Dukhin, S. S.; Shilov, V. N. *Adv. Colloid Interface Sci.* **1980**, *13*, 153–195.
(9) Shilov, V. N.; Borkovskaja, Yu.B.; Budankova, S. N. In *Molecular and Colloidal Electro-optics*; Stoylov, S. P. Stoimenova, M. V., Eds.; Taylor & Francis: New York, 2006; pp 39−57.
(10) Fixman, M. *J. Chem. Phys.* **2006**, *124*, 214506.

all geometries. In a series of theoretical works by Lowenberg and O'Brien[11] and Lowenberg,[12−14] an approximate theory was proposed for the evaluation of the dynamic mobility of dilute suspensions of charged colloidal spheroids and cylinders, valid for axial ratios ($r = a/b$; here a is the semiaxis parallel to the axis of revolution, and b is the semiaxis in the perpendicular direction) in the interval $0.1 \leq r \leq 10$. In addition, it is assumed that the EDL is thin, i.e., its thickness (the Debye length κ^{-1}) is much smaller than the smallest particle dimension.

The same authors provided an expression for a quantity of the utmost importance, namely, the induced dipole coefficient, C: under the action of the alternating field of frequency ω, $\mathbf{E}_0 \exp(-j\omega t)$ ($j = \sqrt{-1}$), an oscillating dipole $\mathbf{d} \exp(-j\omega t)$ is induced in the particle and its double layer that is customarily expressed in terms of the dipole coefficient and the field:

$$\mathbf{d} = 4\pi\varepsilon_0\varepsilon_{rm} ab^2 C\mathbf{E}_0 = 4\pi\varepsilon_0\varepsilon_{rm} ab^2 (C_1 - jC_2)\mathbf{E}_0 \qquad (1)$$

where ε_{rm} is the relative electric permittivity of the liquid medium, and ε_0 is the permittivity of vacuum. As we will see below, the frequency spectrum of the mobility is essentially determined by that of C (a complex quantity, expressed in terms of its real and imaginary components, C_1 and $-C_2$, respectively), together with the inertia of the particles. Frequency relaxations in C are also associated with significant mobility relaxations, hence the importance of the dipole coefficient in any rigorous description of electrokinetics.[15,16] Lowenberg[12−14] provided expressions for the dipole coefficient of spheroids in the (high) frequency range including the Maxwell−Wagner−O'Konski (MWO) relaxation, whereas other expressions were published by Fricke,[17] Sillars,[18] or Saville et al.[19] Recall that such relaxation occurs when the field frequency is so high (typically around a few MHz) that ions in the EDL cannot follow the field oscillations for distances long enough to polarize the double layer by unequal accumulation on the $+z$ and $-z$ sides of the particle (the field is applied in the z direction of a reference frame fixed to the particle center).

These models do not consider the effects of the low-frequency relaxation process or α-relaxation.[20,21] This relaxation (typically in the kHz region) takes place when the phenomenon of concentration polarization cannot occur. We refer to the formation of a gradient of electrolyte concentration around the particle, whereby the salt concentration is increased on one side of the particle and decreased on the opposite, with characteristic distance comparable to the particle dimensions in the field direction. It must be mentioned that its effects are not relevant in electroacoustic measurements, but they become dominant in the dielectric relaxation of the suspensions, a subject that will be dealt with in a forthcoming contribution.

In fact, the problem of the full relaxation spectrum characterization in the case of spheroidal particles was recently solved numerically by Fixman,[10] and analytically by Chassagne and Bedeaux[22] for $\kappa b \geq 1$, a not very restrictive condition, as few practical cases will not fulfill it. These authors proved that their calculations agree with existing data for spheres[23] in the whole frequency range and with the dc mobility calculations previously elaborated on spheroids by O'Brien and Ward[24] for the case of $\kappa b \gg 1$ and dc fields.

All the above-mentioned models assume that the suspensions are dilute. It can be of interest to extend their calculations to account for particle−particle interactions and thus making them applicable to concentrated dispersions. In the case of spheres, cell models have been envisaged and experimentally tested with that purpose.[25,26] Recently, Ahualli et al.[27] presented an approximate analytical model describing the corrections required to take into account hydrodynamic and electrical interactions between particles when the suspensions are moderately concentrated in solids. Although specifically elaborated for spheres, the model is based on such general arguments that it may be safe to apply it to spheroids, at least for not too high (or too low) axial ratios. In fact, its validity has been tested against numerical and analytical calculations, such as those of O'Brien et al.[28]

In this contribution we intend to present new calculations of the dynamic mobility of concentrated suspensions of spheroids. The analytical models elaborated by Loewenberg and O'Brien[11,12] (model I hereafter) and Chassagne and Bedeaux[22] (model II in what follows) will be completed by adding the semianalytical corrections suited to consider finite volume fraction of solids. The results will be compared to each other and to a set of experimental data on the dynamic mobility of concentrated suspensions of elongated goethite (β-FeOOH) particles.

Theoretical Background

In this work we intend to obtain a general expression for the dynamic mobility of concentrated suspensions of spheroidal colloidal particles as a correction to the classical Helmholtz-Smoluchowski equation, valid for particles of any shape, provided the EDL is much thinner than the curvature radius at any point of its surface, and that the surface conductivity is negligible:[29,30]

$$u_e^i = \frac{\varepsilon_{rm}\varepsilon_0\zeta}{\eta_m} f_1^i \cdot f_2^i \cdot f_3^i \qquad (2)$$

where the superscript i ($= \parallel, \perp$) indicates the parallel or perpendicular orientation of the symmetry axis of the particle with respect to the field, ζ is the zeta potential, and η_m is the viscosity of the dispersion medium. The factor f_1 gives information of the inertia effects of the particle due to the oscillating movement, f_2

(11) Lowenberg, M.; O'Brien, R. W. *J. Colloid Interface Sci.* **1992**, *150*, 158–168.
(12) Lowenberg, M. *Phys. Fluids A* **1993**, *5*, 765–767.
(13) Lowenberg, M. *Phys. Fluids A* **1993**, *5*, 3004–3006.
(14) Lowenberg, M. *J. Fluid Mech.* **1994**, *278*, 149–174.
(15) Shilov, V. N.; Delgado, A. V.; Gonzalez-Caballero, F.; Horno, J.; López-García, J. J.; Grosse, C. *J. Colloid Interface Sci.* **2000**, *232*, 141–148.
(16) Ahualli, S; Delgado, A; Miklavcic, S. J.; White, L. R. *Langmuir* **2006**, *22*, 7041–7051.
(17) Fricke, H.; Curtis, H. J. *J. Phys. Chem.* **1937**, *41*, 729–745.
(18) Sillars, R. W. *J. Inst. Electr. Eng.* **1937**, *80*, 378–394.
(19) Saville, D. A.; Bellini, T.; Degiorgio, V.; Mantegazza, F. *J. Chem. Phys.* **2000**, *113*, 6974–6983.
(20) Dukhin, S. S.; Shilov, V. N. *Dielectric Phenomena and the Double Layer in Disperse Systems and Polyelectrolytes*; Wiley: New York, 1974.
(21) Grosse, C. In *Interfacial Electrokinetics and Electrophoresis*; Delgado, A. V., Ed.; Marcel Dekker: New York, 2002; pp 277−327.
(22) Chassagne, C.; Bedeaux, D. *J. Colloid Interface Sci.* **2008**, *326*, 240–253.
(23) DeLacey, E. H. B.; White, L. R. *J. Chem. Soc., Faraday Trans. 2* **1981**, *77*, 2007.
(24) O'Brien, R. W.; Ward, D. N. *J. Colloid Interface Sci.* **1988**, *121*, 402–413.
(25) Lee, E.; Chu, J. W.; Hsu, J. P. *J. Colloid Interface Sci.* **1999**, *209*, 240–246.
(26) Carrique, F.; Cuquejo, J.; Arroyo, F. J.; Jiménez, M. L.; Delgado, A. V. *Adv. Colloid Interface Sci.* **2005**, *118*, 43–50.
(27) Ahualli, S.; Delgado, A. V.; Grosse, C. *J. Colloid Interface Sci.* **2006**, *301*, 660–667.
(28) O'Brien, R. W.; Jones, A.; Rowlands, W. N. *Colloids Surf., A* **2003**, *218*, 89–101.
(29) Lyklema, J. *Foundamentals of Interface and Colloid Science*; Academic Press: London, 1995; Vol. *2*, pp 4.1−4.135.
(30) Arroyo, F. J.; Carrique, F.; Ahualli, S.; Delgado, A. V. *Phys. Chem. Chem. Phys.* **2004**, *6*, 1446–1452.

accounts for the EDL polarization, and f_3 corrects the expression so as to consider finite volume fractions, that is, particle−particle interactions.

The problem is solved for the parallel and perpendicular orientations, and, considering that the orientation of the spheroid will be random, the measured mobility will be given by[31]

$$u_e = \frac{u_e^{\parallel} + 2u_e^{\perp}}{3} \tag{3}$$

This expression can be applied provided the Brownian motion inhibits the tendency of the particles to align in the field direction, a requirement that is achieved if the field strength obeys the following inequality:[32,33]

$${E_0}^2 \ll \frac{k_B T}{\varepsilon_{rm}\varepsilon_0 V} \tag{4}$$

where k_B is the Boltzmann's constant, T is the absolute temperature, and V is the particle volume. For a rod of length 600 nm and maximum cross-sectional diameter 120 nm (the approximate dimensions of our particles) in water and room temperature, this condition requires $E_0 \ll 45$ kV m^{-1}. In our electroacoustic determinations, the applied field ranges between 1 and 12 kV m^{-1}, and hence orientation effects can be neglected in most cases.

Inertia Effects. The inertia effects for a colloidal particle undergoing small amplitude oscillations with angular frequency ω in a viscous incompressible fluid can be taken into account by writing the f_1 functions as follows, in terms of the drag coefficient D_H^i and the added mass M_a^i for each orientation $i = \parallel, \perp$:[10]

$$f_1^i = \frac{D_H^i - j\omega M_a^i}{D_H^i + j\omega M} \tag{5}$$

where M is the particle mass. Expressions for these quantities are provided in Appendix 1.

Contribution of EDL Polarization. This is represented by the factor f_2, which is a function (among other parameters) of the extra conductivity of the fluid due to the existence of an EDL. We restrict ourselves to the main results of the models. For a wider discussion, the reader is referred to the original papers.[11,14] In order to introduce the effects of EDL conductivity and nonzero particle permittivity, Loewenberg[13] derived the following expression (model I):

$$(f_2^i)^I = \frac{1+\lambda_E^2}{1+\tilde{K}_S D^i m_a^i + [(\varepsilon_{rp}/\varepsilon_{rm})m_a^i]\lambda_E^2}, \quad i = \parallel, \perp \tag{6}$$

with $\lambda_E = (1-j)(\varepsilon_{rm}\varepsilon_0\omega/K_m)^{1/2}$, m_a^i as defined in eq A.3, and ε_{rp} being the relative permittivity of the particles. The excess conductivity of the EDL is represented by the dimensionless surface conductivity $\tilde{K}_s = K_s/d^i K_m$, K_m being the conductivity of the dispersion medium, and d^i the minimum particle dimension in the direction perpendicular to the particle motion (minor semiaxis for prolate spheroids in both orientations and oblate spheroids moving perpendicular to their symmetry axis, and major semiaxis for oblate spheroids moving along their symmetry axis). The value of the surface conductivity K_s can be obtained from ζ using the well-known Bikerman equation,[29] which, for a symmetric z-valent electrolyte reads:

$$K_S = \frac{2e^2z^2 10^3 cN_A}{k_B T\kappa}\cdot\left(D^+[\exp(-ze\zeta/2k_BT)-1]\left(1+\frac{3m^+}{z^2}\right) + D^-[\exp(ze\zeta/2k_BT)-1]\left(1+\frac{3m^-}{z^2}\right)\right) \tag{7}$$

where e is the elementary charge, N_A is the Avogadro number, c is the common molarity of ions, $D^{\pm}$ are the diffusion coefficients of the ions, and

$$m^{\pm} = \frac{2\varepsilon_{rm}\varepsilon_0}{3\eta_m D^{\pm}}\left(\frac{k_B T}{e}\right)^2 \tag{8}$$

are the dimensionless mobilities of the respective ions. The expression of the reciprocal Debye length κ is as follows for whatever ionic composition of the liquid medium (N ionic species of valencies z_α, and molar concentrations c_α):

$$\kappa = \left(\frac{\sum_{\alpha=1}^{N} 10^3 N_A c_\alpha e^2 z_\alpha^2}{\varepsilon_{rm}\varepsilon_0 k_B T}\right)^{1/2} \tag{9}$$

In the case of prolate spheroids, the factors D^i in eq 6 are defined for different axial ratios and orientations as (see Appendix 1 for the symbol meaning):

$$D^{\parallel,\perp} = b^3 \frac{F_d^{\parallel,\perp}}{V(1+m_a^{\parallel,\perp})^2} \tag{10}$$

Finally, Lowenberg's calculations also provide a formula for the high frequency value of the dipole coefficient, for the two orientations:

$$(C^{\parallel,\perp})^I = \frac{1}{3}\frac{[(\tilde{K}_S D^{\parallel,\perp}-1)+(\varepsilon_{rp}/\varepsilon_{rm}-1)\lambda_E{}^2](1+m_a^{\parallel,\perp})}{1+\tilde{K}_S D^{\parallel,\perp} m_a^{\parallel,\perp}+(1+m_a^{\parallel,\perp})\varepsilon_{rp}/\varepsilon_{rm})\lambda_E{}^2} \tag{11}$$

As mentioned, Chassagne and Bedeaux[22] carried out a different evaluation of the induced dipole coefficient of a spheroidal particle, based on that of spheres and for monovalent and symmetric electrolyte, both ions having identical diffusion coefficients $D^+ = D^- \equiv D$. Their calculation is valid for arbitrary values of the zeta potential and for $\kappa a \geq 1$.

The proposed expression for the induced dipolar coefficient of a prolate spheroid is (model II):

$$(C^i)^{II} = \frac{K_p^* - K_m^* + 3(1-L^i)[K^{\parallel}+K^U] + 3L^i K^{\perp}}{3K_m^* + 3L^i(K_p^*-K_m^*) + 9L^i(1-L^i)[K^{\parallel}(b/r_0)^3 + K^U(b/r_1)^3 - K^{\perp}]} \tag{12}$$

where the superscript i applies as above, and the meaning of the symbols is explained in Appendix 2. From this, the expression of $(f_2^i)^{II}$ follows:

$$(f_2^{\parallel,\perp})^{II} = 1 - C^{\parallel,\perp}\left(\frac{b}{r_1}\right)^3 \tag{13}$$

(31) Keizer, A.; van der Drift, W. P. J. T.; Overbeek, J. T. G. *Biophys. Chem.* **1975**, *3*, 107–108.
(32) Landau, L. D.; Lifshitz, E. M.; Pitaevskii, L. P. *Electrodynamics of Continuous Media*; Pergamon: Oxford, 1984.
(33) Hunter, R. J. *Foundations of Colloid Science*; Clarendon Press: Oxford, 1984; Vol. *1*.

with

$$r_1 = b + \kappa^{-1}\frac{2.5}{1+2\exp(-\kappa b)} \tag{14}$$

Consideration of Finite Volume Fraction. When the colloidal suspension is not dilute, interactions between particles have to be accounted. We will use an expression obtained for spheres by Ahualli et al.,[27] according to which hydrodynamic and electrical interactions between particles can be accounted for by means of the factor

$$f_3^i = \frac{(1-\phi)}{(1-\phi C^i)(1+\phi\Delta\rho/\rho_m)} \tag{15}$$

where ϕ is the volume fraction of solids, and $\Delta\rho$, the density contrast, is the difference between the particle (ρ_P) and dispersion medium (ρ_m) densities. In this expression, the numerator accounts for the hydrodynamic interactions. The first factor in the denominator ($1-\phi C^i$) includes the electrical interactions between particles, and the second one ($1+\phi\Delta\rho/\rho_m$) ensures that we are referring the particle motions to a zero-momentum frame, as required for the determination of the true mobility from electroacoustic techniques. Note that by electrical interactions we mean those associated with the effect of the field produced by the dipole induced on a given particle (by the external field), on the velocity of a neighbor particle. The reader is referred to the original paper for a wider discussion of the derivation of this expression.

Experimental Section

Materials. Rod-like goethite particles were purchased from Lanxess, USA, under the trade name of Bayferrox-920. As shown in Figure 1, they have uniform shape and moderate polydispersity. Ranges for major and minor semiaxes where $a \in [150-400]$ nm and $b \in [40-60]$ nm, respectively, as obtained from measurements performed on scanning electron microscopy (SEM) pictures. Fitting log-normal distributions to the data we obtained $a = (290 \pm 30)$ nm and $b = (50 \pm 6)$ nm, giving an axial ratio $r = a/b = 5.8 \pm 0.6$. Light scattering techniques were used for obtaining the sizes in situ, using the methods and devices described in ref 2. Dynamic light scattering measurements yielded an average hydrodynamic radius of 190 nm, and a value of 175 nm was obtained as the radius of gyration using static light scattering.

Methods. The powder was first dispersed in deionized and filtered water (Milli-Q Academic, Millipore, France) at a concentration of about 20 g/L. The suspensions were cleaned by successive cycles of centrifugation and redispersion in water. After this cleaning procedure, aqueous suspensions of goethite particles were prepared with different concentrations of the electrolyte (KCl), particle concentrations, and pH values. The suspensions were left to equilibrate for at least 48 h under mechanical stirring. Nevertheless, goethite suspensions with even moderate volume fractions were extremely viscous, as reported by Blakey and James,[34] who explained such behavior by considering that goethite particles tend to flocculate in a similar manner as clay particles in water, because the particles have two types of charged groups on their surface. Such high viscosity made it difficult working with elevated volume fractions or low particle charge conditions, limiting the range of measurements performed to volume fractions up to 8% and pH up to 8.

Dynamic mobility measurements were carried out in an electroacoustic Acoustosizer II device, manufactured by Colloidal Dynamics, Inc. (USA). All measurements were performed at 25.0 ± 0.5 °C.

(34) Blakey, B. C.; James, D. F. *Colloids Surf., A* **2003**, *231*, 19–30.

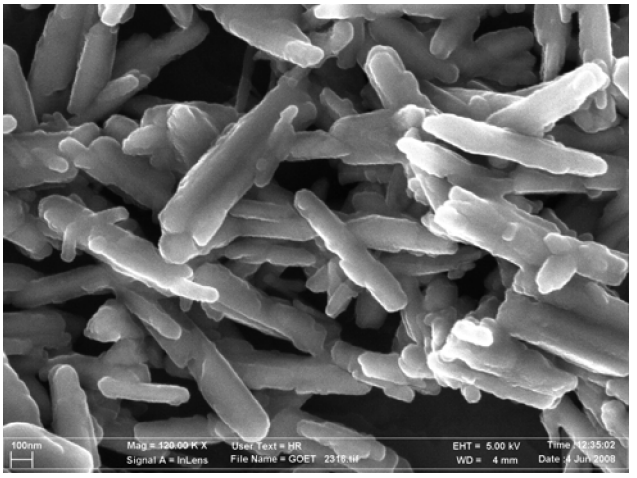

Figure 1. SEM picture of the goethite particles used.

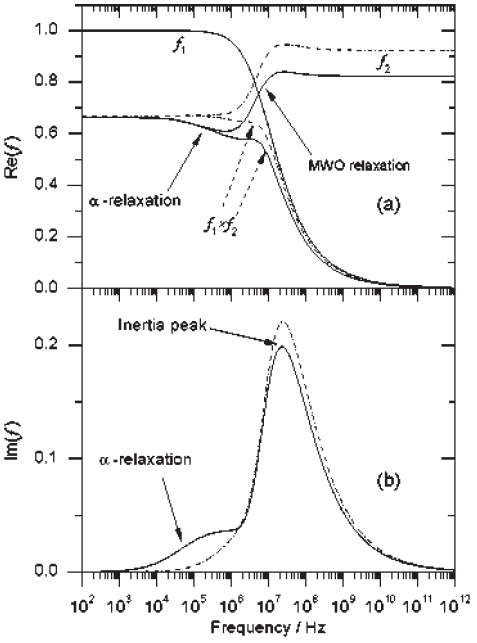

Figure 2. (a) Frequency dependences of the real parts of the functions f_1 (eq 5) and f_2 (according to model I, eq 6, and model II, eq 13) and $f_1 \times f_2$, for prolate particles 100 nm in minor semiaxis and 500 nm in major semiaxis, in a 1 mM KCl solution, with a zeta potential of 100 mV. Dash-dotted lines: model I; solid lines: model II. (b) Same as panel a, but for the imaginary part of $f_1 \times f_2$.

Results and Discussion

Model Predictions. Figure 2 shows the main features of the real parts of the functions f_1, f_2 and their product $f_1 \times f_2$. As observed, f_1 (as above-mentioned, it is the same for both models) displays a single relaxation process (the inertia relaxation), by virtue of which the mobility tends to zero above a certain field frequency ω_i, approximately given by $\omega_i = \nu_m/b^2$ (ν_m is the kinematic viscosity of the solvent), or 14 MHz for the conditions depicted in Figure 2, in good agreement with the model predictions. Note that the relaxation in the mobility is due to the fact that, at such frequencies, there is no time for the electro-osmotic flow of liquid around the particle to fully develop.

The function f_2 is model-dependent, as it describes the polarization of the EDL. The differences between the two models are clear, since model II predicts two relaxations and model I includes only one. This is because the latter does not consider the concentration polarization mechanism,[20,21] unlike model II, even if the approach is based on a simplified theory in this case. The effects of these mechanisms on the mobility spectrum are linked to the fact that concentration polarization reduces the strength of the induced dipole, and hence increases the mobility[15,30] (c.f. eq 1), so that when a certain frequency (the α-relaxation frequency, ω_α) is reached and the process is thus absent, the dynamic mobility decreases. The value of ω_α ($2D^*/b^2$, D^* being the average diffusion coefficient of ions in solution) corresponds to 64 kHz in the case depicted in Figure 2. The α-relaxation appears to be well described by model II, although in any case it does not produce a very significant effect, mainly when compared to the other frequency dependences. For frequencies above α-relaxation, another feature is observed in Figure 2, which is predicted very similarly by both models. This is the so-called MWO relaxation, leading to an increase in the mobility; the process is associated with the decrease in the dipole coefficient because ions cannot move along distances large enough between two successive field oscillations. As a consequence, the polarization of the EDL associated with the conductivity mismatch between particles and medium cannot occur. The relaxation takes place at a frequency $\omega_{MWO} = D^*/\kappa^{-2}$, or 34 MHz, in agreement with the results in Figure 2.

The behavior of the product $f_1 \times f_2$ is a consequence of the three mentioned processes and their relative position in the electroacoustic spectrum. Hence it may appear quite different depending on the suspension properties. In the case shown, the inertia decrease starts before the MWO relaxation takes place, so the characteristic increase associated with this process is masked, and only a small plateau is observed in the real part of the mobility at frequencies above 1 MHz.

The full mobility spectrum, including the factor f_3 (eq 15), is displayed in Figure 3, where both the real and imaginary components of u_e are shown as a function of frequency and volume fraction, for the two models. The effect of f_3 is a decrease in the mobility, a well-known consequence of particle concentration, whereby particles obstruct each other in their movement following the field, and the mobility magnitude is consequently reduced.

An essential point in the comparison between the two models is the evaluation of the effect of axial ratio variations for the case of interest, prolate spheroids in suspension. This has been done in Figure 4, where the dynamic mobility components are plotted for different axial ratios (and fixed minor axis). As observed, the models predict different mobility spectra: at low frequencies, the mobility increases with r in model I, and is not affected by the axial ratio in model II. Above the MWO relaxation (with coincident relaxation frequencies in both approaches), a decreasing trend is observed for both models, although the mobility is systematically larger in model I.

The low-frequency increase of the mobility with r observed in model I is a well-known feature of the mobility of colloidal particles: it increases with the product κl, l being the characteristic size of the particle. Model II does not show this characteristic because of the assumption made in its development: Chasagne and Bedeaux considered that the main contribution to the polarizaton of prolate spheroids comes from ionic motion in the direction of its minor axis, neglecting the effects of conductivity along the major axis. The particle shape, that is to say, the size of the major axis, is accounted for by the depolarization factors

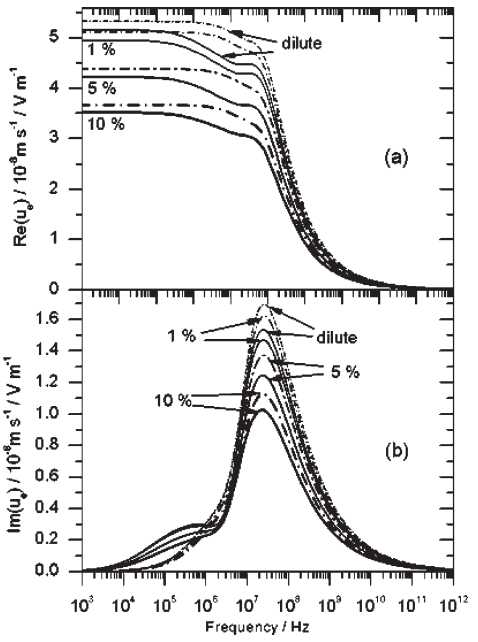

Figure 3. Real (a) and imaginary (b) components of the dynamic mobility of suspensions of prolate particles like in Figure 2, but for particles with a major semiaxis of 1000 nm and different volume fractions, as indicated. Dash-dotted lines: model I; solid lines: model II.

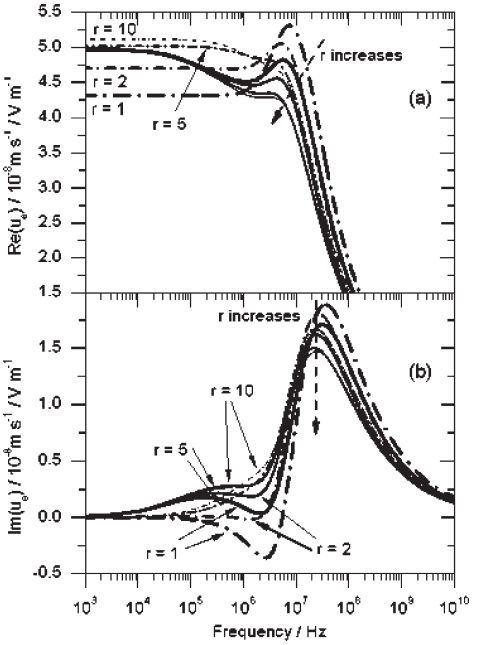

Figure 4. Real (a) and imaginary (b) components of the dynamic mobility of suspensions of prolate spheroidal particles (minor semiaxis b = 100 nm; axial ratio r as indicated) as a function of frequency. Zeta potential: 100 mV; 1 mM KCl solution; volume fraction: 1%. Dash-dotted lines: model I; solid lines: model II.

L^i (see Appendix 2), and only a slight effect comes from this contribution.[22,24]

Overall Behavior of the Dynamic Mobility of Goethite. In Figure 5 we show an example illustrating the main features of the mobility spectrum of prolate goethite particles. The experimental conditions were pH 4, 0.1 mM KCl, and 4% volume fraction. The real part data allows one to appreciate the end of the MWO rise and the start of the inertia decrease. Note that the accuracy of the

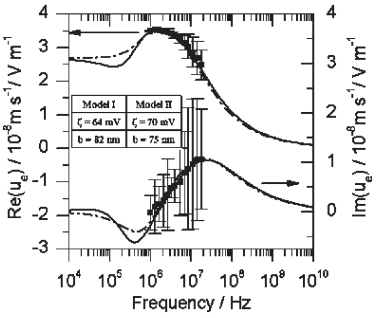

Figure 5. Real and imaginary components of the dynamic mobility spectrum in a goethite suspension containing 4% volume fraction of solids, in a 0.1 mM KCl solution at pH 4. Experimental data are shown together with the predictions of models I and II; the best fit parameters (zeta potential and short semiaxis) are shown in the inset. Dash-dotted lines: model I; solid lines: model II.

real part is much higher than that of the imaginary component (compare the size of the error bars) because of the small values of the phase angle characteristic of these systems. Also, the accuracy is better at low than at high frequencies, and hence the main weight of the fitting will be associated with the real part, especially in the low-frequency side of the spectrum. In all cases, the fitting was performed by the weighted least-squares method, using the zeta potential ζ and the short semiaxis b as parameters, whereas the axial ratio was fixed to 5.8, the value obtained from SEM pictures. Note that, although model I is not strictly applicable because of the low values of κb (typically around 3), the two approaches are capable of properly fitting the data, with negligible differences in either the zeta potential or the axis dimensions. These considerations apply to all the obtained data. In the following, in order to present the results more clearly, we will not include the error bars in the plots, but we have found that the relative errors are in all cases similar to those shown in Figure 5.

Effect of Volume Fraction. As depicted in Figure 6, both the real and imaginary components of the mobility are reduced by increasing particle volume fraction, as theoretically predicted. However, neither of the models can account properly for the observed trends of the experimental data. The best-fit parameters shown in Table 1 indicate that a slight decrease in both ζ and b with volume fraction is required to fit the data.

This apparent inconsistency must be related to the model used to account for the interactions, strictly applicable to monodisperse, uniformly charged spheres. We already mentioned the tendency of concentrated suspensions of elongated goethite particles to be flocculated, partly due to the fact that the charge on the particle surface can be different (even in sign) for different crystal faces, a situation impossible to take into account in the frequency domain, the only approaches having been elaborated for dc data.[35] Nevertheless, it is possible to use the data presented in Table 1 in order to obtain average values of ζ and b, which might be considered representative of goethite in 0.5 mM KCl and pH 4 for the whole range of volume fractions.

It is also worth pointing out an additional feature of the data in Figure 6. This is the change in tendency indicated by the dash-dotted arrows: small plateaus are observed in the real part (and shoulders in the imaginary component). These are presumably related to the fact that the MWO process takes place for frequencies comparable to those corresponding to the inertial decay. Finally, it is necessary to mention that the fits do not properly reproduce the high frequency decrease: the tendency to flocculation of our systems should give rise to an increase in its actual polydispersity, leading to a wider inertial decay in the electroacoustic spectra.

(35) Velegol, D.; Anderson, J. L.; Solomentsev, Y. In *Interfacial Electrokinetics and Electrophoresis*; Delgado, A. V., Ed.; Marcel Dekker: New York, 2002; pp 147−172.

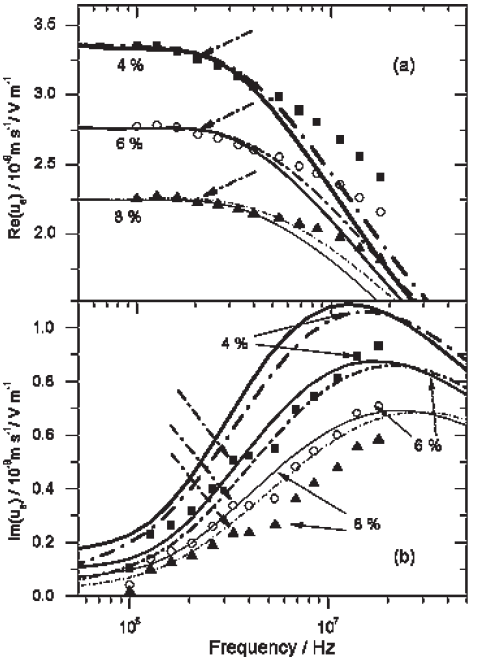

Figure 6. Same as Figure 5, but in a 0.5 mM KCl solution and for different volume fractions, as indicated. (a) real component of the mobility; (b) imaginary component. The best-fit parameters (model I, dash-dotted lines; model II, solid lines) are shown in Table 1.

Table 1. Best-Fit Values of the Zeta Potential ζ and the Minor Semiaxis b Corresponding to the Data in Figure 6[a]

	ζ/mV		b/nm	
volume fraction ϕ/%	model I	model II	model I	model II
4	64	70	97	113
6	56	61	80	92
8	48	52	67	77

[a] Electrolyte concentration 0.5 mM KCl; pH 4.

Dynamic Mobility and Ionic Strength. Figure 7 displays the effect of the ionic strength on the dynamic mobility (only the real part will be considered, according to our comments above concerning accuracy) of a suspension with 4% volume fraction of goethite particles and pH 4. The best-fit parameters to models I and II are detailed in Table 2. The real part of the mobility undergoes a decrease when the salt concentration is increased, and the data in Table 2 demonstrate that this decrease manifests in a decline in zeta potential with KCl concentration, the expected EDL compression behavior when the concentration of an indifferent electrolyte is raised. Such a reduction in zeta gives rise to a more likely aggregation between particles, this in turn yielding a larger mean size. This may explain the trend of the inertia relaxation frequency toward lower values, displayed in Figure 7. We note that both models describe the data with great accuracy, and, for the conditions of our experiments, they are absolutely compatible, and they can both be used with confidence for obtaining the zeta potential of elongated particles from their dynamic mobility spectrum.

Concerning the MWO rise of the real part of the dynamic mobility, the Figure indicates that it is clearly reduced until becoming unobservable when the ionic strength is increased. The explanation of such a decrease in the amplitude of the

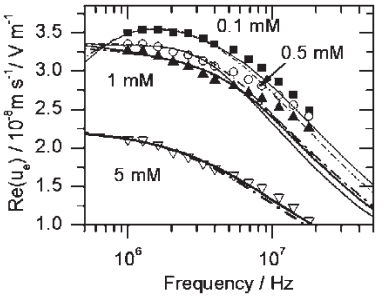

Figure 7. Effect of ionic strength (KCl concentration) on the dynamic mobility of goethite particles in a suspension containing 4% of solids by volume. The pH is 4. The best-fit parameters (model I, dash-dotted lines; model II, solid lines) are shown in Table 2.

Table 2. Best-Fit Values of the Zeta Potential ζ and the Minor Semiaxis b Corresponding to the Data in Figure 7[a]

	ζ/mV		b/nm	
ionic strength (KCl mM)	model I	model II	model I	model II
0.1	64	70	82	75
0.5	64	70	97	113
1	59	64	86	96
5	35	35	108	103

[a] Volume fraction: 4%; pH 4.

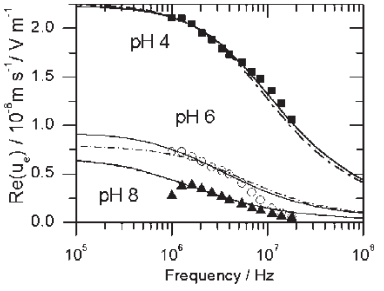

Figure 8. Real component of the dynamic mobility of goethite particles as a function of the frequency of the field, for the pH values indicated. In all cases, the KCl concentration in the medium is 5 mM, and the volume fraction of solids is 4%. The best-fit parameters (model I, dash-dotted lines; model II, solid lines) are shown in Table 3.

MWO process comes from two facts. One is the already mentioned trend of the inertia relaxation toward lower frequencies, partly masking the MWO process. The second reason can be understood from the observation that the surface conductivity K_S of the particles plays a decreasing role on their electrokinetics when K_m is increased (for instance, in eq 6 $\tilde{K}_s = K_s/d^i K_m$ is the quantity that matters). This makes the induced dipole coefficient more negative and closer to its high frequency value, so that the importance of the MWO relaxation is diminished.

The Effect of pH. Finally, Figure 8 shows the real component of the dynamic mobility of suspensions at pH 4, 6, and 8, and with a 4% volume fraction of solids in 5 mM KCl. As before, the lines correspond to the fittings performed using the two models, with the parameters displayed in Table 3. Note that the positive mobility decreases when the pH is increased in the 4−8 range for all frequencies. This is a clear indication that goethite has an isoelectric point above pH 8, and in fact other reported results[34,36,37] indicate a value around pH 9. Again, both models predict very similar mobility trends, and the tendency of aggregation expected when the isoelectric point is approached manifests in a reduction of the frequency of the inertia relaxation, associated with a larger average particle size.

Table 3. Best-Fit Values of the Zeta Potential ζ and the Minor Semiaxis b Corresponding to the Data in Figure 8[a]

	ζ/mV		b/nm	
pH	model I	model II	model I	model II
4	35	35	108	103
6	12	14	146	194
8	10	10	283	291

[a] Volume fraction: 4%; ionic strength: 5 mM KCl.

Conclusions

The main aim of this work was to elaborate on models of the electrokinetics of elongated particles in ac fields. We have considered shape and zeta potential effects, as well as the influence of volume fraction on the dynamic mobility of prolate spheroids. Two theoretical models (differing in their description of the double layer polarization mechanisms) suited to dilute suspensions (but not compared before to each other) have been modified to account for the finite volume fraction of solids. The two approaches have been used to obtain the zeta potential and average dimensions of elongated goethite particles. It has been found that for the range of dimensions and zeta potentials of our particles, and in the frequency interval experimentally accessible, the models give a limited account of the observed trends of the experimental data with volume fraction. Fitting of the data requires allowing the zeta potential and particle dimensions to change with the volume fraction. This is manifestation of the fact that goethite particles have a great tendency to flocculate, partly due to the inhomogeneity (even in sign) of the charge distribution on the particle surface. On the contrary, regarding the effects of ionic strength and pH on the dynamic mobility, the two models perform with a great accuracy, and lead to a coherent characterization of the particle dimensions and surface potential.

Acknowledgment. Financial support from Junta de Andalucía, Spain (Project PE-2008-FQM-3993) and ESF (Cost Action D43) is gratefully acknowledged.

Appendix 1

Lawrence and Weinbaum[38] proposed the approximate formula

$$D_H^i = -\eta d^i \left[F_0^i + \lambda^i F_d^i + (\lambda^i)^2 \frac{M_a^i}{\rho_m (d^i)^3} + \left(\frac{(F_0^i)^2}{6\pi} - F_d^i \right) \frac{\lambda^i}{1+\lambda^i} \right] \quad \text{(A.1)}$$

for the drag coefficient of an ellipsoid, where

$$\lambda^i = (1-j)\sqrt{\frac{\omega (d^i)^2}{2\nu_m}} \quad \text{(A.2)}$$

The other quantities are given for both prolate and oblate spheroids in refs 12 and 13, but here we will focus on the case

(36) Antelo, J.; Avena, M.; Fiol, S.; López, R.; Arce, F. *J. Colloid Interface Sci.* **2005**, *285*, 476–486.
(37) Allison, S. *J. Colloid Interface Sci.* **2009**, *332*, 1–10.
(38) Lawrence, C. J.; Weinbaum, S. *J. Fluid Mech.* **1988**, *189*, 463–489.

of prolate particles ($r > 1$), like the ones we used in our experiments:

Added mass ($M_a^{\parallel,\perp}$; in dimensionless form, $m_a^{\parallel,\perp}$):

$$m_a^{\parallel} = \frac{M_a^{\parallel}}{\rho_m V} = \frac{1}{r}\frac{\sqrt{r^2-1} - r\cosh^{-1}(r)}{\cosh^{-1}(r) - r\sqrt{r^2-1}}$$
$$m_a^{\perp} = \frac{M_a^{\perp}}{\rho_m V} = \frac{1}{1+2m_a^{\parallel}} \tag{A.3}$$

Steady Stokes resistance:

$$F_0^{\parallel} = 4\pi r \frac{1+m_a^{\parallel}}{1/2 + r^2 m_a^{\parallel}}$$
$$F_0^{\perp} = 8\pi r \frac{1+m_a^{\parallel}}{3/2 + r^2 m_a^{\parallel}} \tag{A.4}$$

Basset force:

$$F_d^{\parallel,\perp} = (1+m_a^{\parallel,\perp})^2 I_{\parallel,\perp} \tag{A.5}$$

with:

$$I_{\parallel} = 2\pi r^2 \left(\frac{r^2-2}{(r^2-1)^{3/2}} \cos^{-1}\left(\frac{1}{r}\right) + \frac{1}{r^2-1} \right)$$
$$I_{\perp} = \pi \left(\frac{r^4}{(r^2-1)^{3/2}} \cos^{-1}\left(\frac{1}{r}\right) + \frac{r^2-2}{r^2-1} \right) \tag{A.6}$$

Appendix 2

The quantities appearing in eq 12 defining the dipole coefficient have the following meanings and expressions:

Complex conductivities of bulk electrolyte and particles:

$$K_m^* = K_m + j\omega\varepsilon_{rm}\varepsilon_0$$
$$K_p^* = j\omega\varepsilon_{rp}\varepsilon_0 \tag{A.7}$$

Complex conductivities associated with fluxes of ions along or perpendicular to the surface of the particle in the EDL:

$$K^{\parallel} = -K_m I_{n,eq} - \frac{2J_1 K_m [I_{c,eq}{}^2 - I_{n,eq}{}^2]}{J_2 (r_0/b)^3 \exp[\lambda_n (r_0 - b)]}$$
$$K^{\perp} = \frac{2J_1 K_m I_{n,eq}}{J_2 (r_0/b)^3 \exp[\lambda_n (r_0 - b)]} \tag{A.8}$$

where:

$$I_{n,eq} = \frac{-1}{b^2}\int_b^{r_0} x \left[\cosh\left(\frac{e\Psi_{eq}}{k_B T}\right) - 1 \right] dx$$
$$I_{c,eq} = \frac{1}{b^2}\int_b^{r_0} x \left[\sinh\left(\frac{e\Psi_{eq}}{k_B T}\right) \right] dx$$
$$r_0 = b + \kappa^{-1}\left(1 + \frac{3}{\kappa b}\exp(-e\zeta/2k_B T)\right) \tag{A.9}$$

In these integrals $\Psi_{eq}(r)$ is the equilibrium electric potential at distance r of the center of a spherical particle of radius b, and $x = (r - b)$. Other parameters needed are

$$\lambda_n = \sqrt{\frac{j\omega}{D}} \tag{A.10}$$

$$J_1 = 1 + \lambda_n r_0 \tag{A.11}$$

$$J_2 = 2 + 2\lambda_n b + \lambda_n{}^2 b^2 \tag{A.12}$$

For prolate spheroids, the depolarization factors can be written as follows:

$$L^{\parallel} = \frac{1}{1-r^2} + \frac{r}{(r^2-1)^{3/2}} \ln(r + (r^2-1)^{1/2})$$
$$L^{\perp} = \frac{1 - L^{\parallel}}{2} \tag{A.13}$$

Finally, the correction for the fluid movement is introduced by introducing in eq 12 the quantity[39]

$$K^U = -K_m m \frac{e\zeta}{k_B T} I_{c,eq} \left[\frac{I_{n,eq} - \gamma I_{c,eq} - 1/4}{(I_{n,eq} - \gamma I_{c,eq}) - J_2/(2J_1)(r_0/b)^3 \exp(\lambda_n (r_0 - b))} - 1 \right]$$
$$(\gamma = I_{n,eq}/I_{c,eq}) \tag{A.14}$$

(39) Note the missing minus sign at the beginning of this expression in the original paper.